Stem Cell Research & Therapy

RESEARCH

Open Access

Mesenchymal stem cells overexpressing neuropeptide S promote the recovery of rats with spinal cord injury by activating the PI3K/AKT/GSK3β signaling pathway

Wenhui Yang[1,2,3,4†], Yilu Li[1,2,3†], Yushi Tang[1,2,3†], Zhenxing Tao[1,2,3], Mengyuan Yu[1,2,3], Cuiping Sun[1,2,3], Yang Ye[1,2,3], Bai Xu[1,2,3], Xudong Zhao[1,2,3], Yazhuo Zhang[5*] and Xiaojie Lu[1,2,3*]

Abstract

Background Transplantation of nasal mucosa-derived mesenchymal stem cells (EMSCs) overexpressing neuropeptide S (NPS) is a promising approach for treating spinal cord injury (SCI). Despite the potential of stem cell therapy, challenges remain regarding cell survival and differentiation control. We aimed to conduct orthotopic transplantation of transected spinal cord to treat rats with complete SCI.

Methods In this study, we loaded NPS-overexpressing EMSCs onto hydrogels to enhance cell survival in vivo and promote neuronal differentiation both in vitro and in vivo. However, in vitro co-culture promoted greater neuronal differentiation of neural stem cells ($P < 0.01$). When transplanted in vivo, NPS-overexpressing EMSCs showed greater cell survival in the transplanted area compared with stem cells without gene modification within 4 weeks after spinal cord implantation in rats ($P < 0.01$).

Results Compared with those in the other groups, stable overexpression of NPS-EMSCs in a rat model with SCI significantly improved the treatment effect, reduced glial scar formation, promoted neural regeneration and endogenous neural stem cell proliferation and differentiation into neurons, and improved motor function.

Conclusions These results indicate that this effect may be achieved by the overexpression of NPS-EMSCs through the activation of the PI3K/Akt/GSK3β signaling pathway. Overall, the overexpression of EMSCs significantly improved the therapeutic effect of SCI in rats, strongly supporting the potential for gene modification of mesenchymal stem cells in clinical applications.

†Wenhui Yang, Yilu Li and Yushi Tang contributed equally to this work.

*Correspondence:
Yazhuo Zhang
zyz2004520@163.com
Xiaojie Lu
9862019541@jiangnan.edu.cn

Full list of author information is available at the end of the article

Keywords Neuropeptide S, Nasal mucosa mesenchymal stem cells, Transected spinal cord injury, PI3K/Akt/GSK3β pathway, Neural stem cells

Background

Spinal cord injury (SCI) is a serious form of nerve dysfunction usually caused by trauma, resulting in total or partial loss of nerve function. Due to the absence of effective treatments, SCI is a devastating disease that can be fatal [1].

The limited therapeutic efficacy for SCI is primarily due to pathological events following the injury, including extensive neuronal and glial cell death, lack of neurotrophic factors, accumulation of inhibitory myelin fragments, glial scarring due to immune cell infiltration and reactive astrocyte proliferation, and a microenvironment at the site of SCI injury that is not suitable for nerve regeneration [2–5].

Mesenchymal stem cells can reduce inflammation and apoptosis at the site of injury, secrete neurotrophic and nerve growth factors, and promote axon regeneration and nerve pathway reconstruction, all of which offer significant advantages for SCI repair [6–9]. A significant number of mesenchymal stem cells, known as nasal mucosal mesenchymal stem cells (EMSCs), are present in the lamina propria of the nasal mucosa, derived from the neural crest, and retain the potential for multidirectional differentiation and self-renewal [10–12]. Compared with other mesenchymal stem cells, they have the advantages of simple material and minimal impact on donors, easy isolation, and in vitro culture because they can be provided directly by donors and, therefore, raise no ethical concerns [13, 14]. Additionally, EMSCs demonstrate a high safety profile, with no genetic variation after extensive in vitro passage by chromosomal and tumor gene analyses [15–17]. These characteristics make EMSCs a promising cell type. Previous studies have shown that EMSCs transplantation can promote SCI repair to some extent [18, 19]. However, cell transplantation has several disadvantages, including the harsh microenvironment following SCI, which makes it difficult for transplanted cells to survive and grow in injured areas [20]. Studies have shown that genetic engineering techniques have been used to introduce neurotrophic genes into seed cells, which are then transplanted for the treatment of SCI. These findings indicate that such modifications can promote injury repair functions in these cells [21]. Therefore, genetic engineering is used to modify DNA at the molecular level. Exogenous genes are transferred into the genetic material of cells through vectors, and such genes can be replicated, transcribed, and translated within the cells. With advancements in gene therapy research, its application to SCI has rapidly progressed [22, 23].

In 2002, neuropeptide S (NPS), which consists of 20 amino acids, was identified through reversal pharmacology as an endogenous ligand for the orphan receptor GPR154 (also known as GPRA or VRR1) [24]. NPS and their receptors are derived from shorter precursor proteins [25]. The gene sequences encoding these precursors are highly conserved in vertebrates but absent in the genomes of fish and invertebrates. This evolutionary distribution suggests that these genes may perform specific physiological functions [26, 27].Central exogenous NPS has been shown to enhance locomotor activity in rodent studies. The NPS receptor (NPSR) is produced in brain regions associated with locomotion, including the basal ganglia. Furthermore, NPS mediates dopaminergic neurotransmission, indicating that endogenous brain NPS plays a role in the regulation of locomotion [28]. Previous studies have shown that NPS can produce nociceptive effects at the spinal cord level in mice, acting through NPSR [29]. Therefore, we hypothesized that transplantation of NPS-modified stem cells into damaged spinal cords would promote axon regeneration and functional recovery after SCI.

Fibrin hydrogels, created through the polymerization of fibrin monomers into a fibrous three-dimensional (3D) structure, serve as innovative scaffolds that play an important role in blood clotting during the natural wound healing process. They are commonly used in tissue engineering because of their biocompatibility, structural similarity to native tissues, transport and tunable properties, and ability to deliver drugs and growth factors.

In summary, we aimed to construct EMSCs that overexpress NPS using recombinant adenoviral technology and load them onto fibrin scaffolds to observe their effects on axonal regeneration in a rat model with transected SCI.

Materials and methods

Animals

In this study, we utilized 72 female Sprague–Dawley (SD) rats (6 weeks old, 150–180 g) and one pregnant SD rat (350 g, 14 days gestation), all purchased from Spover Biotechnology Co., Ltd. (Suzhou, China). The rats were housed in cages (three rats per cage) at a temperature of 22 °C, humidity of 55%, 12-hour light-dark cycles, and free access to food and water. Animal euthanasia was carried out by anesthetizing the rats using inhaled isoflurane (Qingdao Orbiepharm Co., Ltd.) at a concentration of 3–4% for 2–3 min until they were fully anesthetized. After confirming the absence of positive reflexes, cervical

spine dislocation was performed, and they were euthanized. The deceased animals were placed in body bags and sent to the experimental animal center for centralized processing.

Isolation and expansion of rat EMSCs

EMSCs were isolated according to the protocol described in a previous study [30]. Two female SD rats were euthanized following isoflurane anesthesia, and tissue samples were obtained from the lower third of the nasal septum mucosa. The mucous membranes were carefully cut into small pieces (0.5–1 mm^3) and placed in DMEM/F12 medium (HyClone) containing 10% fetal bovine serum (Gibco; A5670701) and penicillin-streptomycin (100 U/ml). This mixture was transferred to a humidified incubator with 5% CO_2 at 37 °C. The medium was changed by 50% on day three, completely replaced on day seven, and non-adherent cells were eliminated. Adherent EMSCs were expanded and purified through three passages after initial inoculation. The culture medium was adjusted based on cell condition, and the cells were observed every 3 days using an inverted phase-contrast microscope. After a period of 14 days, adherent EMSCs were subjected to digestion using 0.25% trypsin and subsequently subcultured until they reached 80–90% confluence. EMSCs were identified by detecting the expression of Nestin (Affinity; DF7754), vimentin (ABclonal; A21648), CD44 (ABclonal; A24023), and SOX2 (Proteintech; 11064-1-AP) and subjected to immunofluorescence staining according to the protocol described in the following section.

Construction of recombinant adenovirus

The NPS gene sequences were synthesized as follows: forward, CGCAAATGGGCGGTAGGCGTG; reverse, GAAATTTGATGCTATTGC. We prepared pcADV-EF1-mScarlet-CMV-Nps-3FLAG by inserting the NPS gene into the vector, and the GL2004 pcADV-EF1-mScarlet-CMV-MCS-3xFLAG vector was used as the parallel group. Recombinant NPS adenovirus shuttle plasmid was obtained from Heyuan Biotechnology (Shanghai, China). EMSCs were infected with adenovirus vectors, and 48 h post-inoculation, the transfected NPS EMSCs were imaged using fluorescence microscopy (Zeiss, Germany) and validated by western blot analysis to detect NPS (CLOUD-CLONE-CORP; PAA796Ra01) expression. EMSCs overexpressing NPS were named NPS-EMSCs, and those transfected in parallel were named ADV-EMSCs.

RNA sequencing and transcriptome analysis

For further evaluation, RNA sequencing techniques were used to investigate the relevant signaling pathways activated by the introduction of NPS into EMSCs. Total RNA was extracted from the EMSCs and NPS-EMSCs using TRIzol reagent (Invitrogen; 15596-026). RNA samples from the EMSCs and NPS-EMSC groups were sequenced by Oebiotech Co., Ltd. (Shanghai, China) using an Illumina Nova6000 platform to generate 150-bp paired-end reads. The raw data (fastq format) were processed using Trimmomatic to remove low-quality reads and retain clean reads. DESeq software [31] was used to calculate each sample to analyze the differentially expressed genes (DEGs) according to the different multiples and the test results of the significance difference. The criteria for screening DEGs included a P value < 0.05 and fold change > 2. Based on the hypergeometric distribution algorithm, the GO [32], KEGG [33] Pathway, Reactome, and WIKIPATHWAY enrichment analyses of the DEGs were used to screen for entries with significant enrichment functions. R (v 3.2.0) was used to create column, chord, and enrichment analysis circle diagrams for significantly enriched function entries. GSEA software was used for gene set enrichment analysis.

Preparation of fibrin hydrogels

A fibrinogen solution with a concentration of 100 mg/mL in phosphate-buffered saline (PBS) was prepared and subsequently mixed with an equal volume of thrombin solution at a concentration of 20 U/mL in PBS. The final fibrinogen concentration was 50 mg/mL, and the resulting hydrogel scaffold was used for subsequent experiments. After vacuum freeze-drying, the morphology of the hydrogel scaffolds was analyzed using SEM. The viability of the EMSCs cultured on the scaffolds was assessed by AM/PI staining. EMSCs (1×10^5) were seeded in 24-well plates and incubated for 5 days. The cells were stained for 30 min at room temperature in the dark using a working staining solution for live/dead cells (Apex Bio; K2247). The staining solution was removed, and the cells were photographed under a fluorescence microscope (Zeiss, Germany). The number of viable cells was quantified using ImageJ software.

In vitro differentiation assay

EMSCs and NPS-EMSCs were seeded in 6-well plates at a density of 5×10^5 cells/well in 2 ml of DMEM/F12 medium containing 10% FBS per well. At 80% confluence, adipogenesis and osteogenic differentiation were induced using adipogenesis and osteogenic induction media, respectively. Differentiation induction medium was administered every 3 to 4 days. Following a 21-day differentiation period, Oil Red O (Sigma-Aldrich; 1320-06-5) and alkaline phosphatase (source leaf; S10090-1 mg) staining were performed to evaluate adipogenesis and osteogenesis, respectively.

Surgical procedures

Modified EMSCs were loaded onto the hydrogel to evaluate their effect on rats with complete transverse SCI. The rats were randomly divided into the following groups: injury, fibrin hydrogel transplantation, EMSCs loaded hydrogel, NPS-EMSCs loaded hydrogel, and sham operation groups. Anesthesia was induced using inhaled isoflurane (3–4% concentration) through a face mask for 2–3 min and then adjusted to 2–3% to maintain anesthesia. The rats were placed prone on an operating table, their limbs immobilized, and their backs shaved and disinfected with iodophor. A longitudinal incision along the spinous process at T8 was made to separate the soft tissue, resect the corresponding lamina, and expose the spinal cord. A 2 mm long section of the T8-T9 spinal cord was excised under a microscope using micro scissors. After the injury, an appropriate amount of hemostatic sponge was applied to control the bleeding, and the hydrogel stent was transplanted to the injury site. The wound was sutured, and the dissected spinal meninges, muscle, and skin layers were carefully closed. After disinfection, the rats were transferred to a 37℃ thermostat and observed until they recovered from anesthesia. In the sham group, only the thoracic plates were removed and then closed. Antibiotic injections were administered daily for 1 week postoperatively to prevent infection, and the rats were manually emptied twice daily until spontaneous urination resumed.The study's conduct and findings were reported in accordance with the ARRIVE Guidelines 2.0, ensuring rigorous and transparent reporting of our animal-based research.

Co-culture with neural stem cells (NSCs)

Following anesthesia, pregnant rats (15–16 days gestation) were taken, and fetal mice were removed from their abdomen. The fetal mice were sterilized by soaking in 75% ethanol and then transferred to a sterile pre-chilled PBS solution. A fetal mouse brain was dissected, and the attached meninges and blood vessels were removed. The cerebral cortex was isolated, and the cortical meninges were peeled. The resulting tissue was transferred to a 5 mL of 0.125% trypsin centrifuge tube and digested in an incubator at 37 °C for 15 min, gently shaking the mixture every 5 minutes. The digested tissue was centrifuged at 1200 rpm for 15 min, the supernatant was discarded, and the resulting pellet was washed three times in sterile PBS. The supernatant was further discarded, and 2 mL of NSCs medium was added [34]. The cell suspension was then collected in fresh centrifuge tubes. After 3–4 repetitions, the tissue was completely digested, and the cell suspension was filtered for collection. NSCs were seeded in flasks (1×10^6 cells) and cultured in an NSCs medium. After 7 days of culture, the NSCs (1×10^5/well) were placed in the lower layer of a 24-well transwell of polylysine-coated (Gibco; A3890401)-treated crawlers, NPS-EMSCs (1×10^5/well) were cultured in a 24-well transwell insert chamber (0.4 μm diameter), and NSCs and NPS-EMSCs were cultured using NSCs medium, and after 72 h, with EdU kit (Apex Bio; K1075). NSCs (1×10^5/well) obtained in the first step were further placed in the lower layer of a 24-well transwell lined with polylysine-treated crawlers, NPS-EMSCs (1×10^5/well) were cultured in a 24-well transwell insert chamber (0.4 μm diameter), and NSCs and NPS-EMSCs were cultured using Neurobasal medium (Gibco;10888022) containing 2% B27 and treated with AKT inhibitors(MCE; HY-10358). Immunofluorescence was used to detect the effect of NPS-EMSCs on NSC differentiation 72 h after induction.

Immunofluorescence

In vitro-cultured cells were fixed with 4% paraformaldehyde. In vivo-cultured spinal cord segments from T8-T9 were fixed with 4% paraformaldehyde and immersed in 20% and 30% sucrose. The sections were then cut into 15 μm thick sections via a cryostat (Leica Microsystems). For immunofluorescence staining, the samples were blocked in 5% bovine serum albumin (BSA) and 0.3% Triton X-100 for 30 min at room temperature and then incubated overnight at 4 °C with primary antibodies, including GFAP (Proteintech; 60190-1-Ig), Tuj-1 (Proteintech; 66375-1-IG), MAP2 (Proteintech; 17490-1-AP), and MBP (Proteintech; 10458-1-AP). DAPI (Invitrogen; YD3918381) was used for nuclear staining. Samples were incubated with secondary antibodies for 1 h at room temperature before nuclear staining. Images were acquired using a confocal microscope (Zeiss, Germany).

Western blotting

According to the manufacturer's guidelines, the cells were lysed using a buffer that included a protease (Beyotime Biotechnology; P1005) and a phosphatase inhibitor (MCE; HY-L081). After protein extraction, concentrations were measured using a BCA protein assay kit (Cwbiotech; CW0014). Proteins were separated using 8%, 10%, and 15% sodium dodecyl sulfate-polyacrylamide gel electrophoresis and transferred to PVDF membranes (Millipore). The membranes were blocked with 5% skim milk powder (BD; 232100) for 2 h, and the primary antibody was applied on a 4 °C horizontal shaker overnight. Furthermore, the secondary antibody (Cwbiotech; CW0102, CW0103) was applied for 1 h at room temperature. Antibodies used included anti-GAPDH (Servicebio; GB11002-100), anti-PI3K (CST;4249), anti-phospho-PI3K (positive biological;310164), anti-AKT (CST;4691T), anti-phospho-AKT (CST;4060T), anti-GSK3β (Proteintech;22104-1-AP), and anti-phospho-GSK3β (Proteintech;67558-1-IG). Protein bands were

visualized using an enhanced chemiluminescence kit (Apex Bio; K1233).

HE staining

The spinal cord segments were fixed in 4% paraformaldehyde 12 weeks post-surgery, subsequently embedded in paraffin, and sectioned into 5 μm slices for hematoxylin and eosin (H&E) staining. The distance between the severed ends of the spinal cord was measured and analyzed.

Beattie & Bresnahan motor rating (BBB) scale score

The locomotor function of rats was evaluated utilizing the BBB score [35]. Sequential recovery stages were identified through scores ranging from 0 to 21 on various evaluation indices, which included joint motion, stepping ability, coordination, and trunk stability. Scores and recovery stages were positively correlated. The rats were closely observed while permitted to roam freely for 5 min during the testing process, and the group identities were kept confidential from the observers during the test.

Statistical analysis

GraphPad Prism (GraphPad, San Diego, CA, USA) and Adobe Illustrator 2023 (Adobe, San Jose, CA, USA) were utilized for the generation of graphs. Quantitative analysis of immunofluorescence (IF) images was conducted using ImageJ software (Wayne Rasband, National Institutes of Health). The term biological replicates of experiments that were performed a minimum of three times, unless otherwise specified. A one-way analysis of variance (ANOVA) was employed to assess significant differences between groups. Data are presented as means ± standard deviations (SDs), with error bars indicating SDs ($^{*}P < 0.05$, $^{**}P < 0.01$, $^{***}P < 0.001$). The significance level was set at $P < 0.05$.

Results

Effectiveness of NPS transgene expression

Immunofluorescence was used to evaluate the success of recombinant adenovirus-transfected EMSCs overexpressing NPS. Compared with the EMSCs group, the NPS-EMSCs emitted mScarlet red fluorescence under a fluorescence microscope 48 h post-transfection with the recombinant adenovirus (Fig. 1a), and the images revealed that over 90% of the cells were mScarlet-positive (Fig. 1b), indicating successful transfection. Western blotting was used to assess NPS expression levels, and the results were consistent with the immunofluorescence findings (Fig. 1c). NPS expression was significantly higher in the NPS-EMSCs group compared with other groups (Fig. 1d).

RNA sequencing reveals changes in the gene expression profiles of NPS-EMSCs

TRIzol was used to extract total RNA for sequencing to further identify changes in gene expression in cultured NPS-modified EMSCs. Total RNA was extracted from EMSCs as a control for DEGs, of which 1,341 were downregulated and 1,120 were upregulated (Fig. 2a). Functional pathway enrichment analysis was performed using the Gene Ontology (GO) database. In the biological function category, cell adhesion and axonal guidance, mainly enriched in gene expression, were the main pathways. In the molecular function category, notable enrichments were observed in the following: ion channel activity, extracellular matrix structural components, growth factor activity, fibronectin binding, and collagen binding. For the enrichment of cellular component categories, we identified neuronal cell bodies, axons, cell surfaces, extracellular matrix, and basement membranes (Fig. 2b, c, d). After the DEGs were identified, KEGG (primary public pathway database) enrichment analysis was performed, and combined with the annotation results. KEGG revealed 20 significant pathways changes compared with those in NPS-EMSCs and EMSCs (Fig. 2e). Wiki Pathway Enrichment Top20 analysis revealed that EMSCs overexpressing NPS could be promising for the treatment of SCI (Fig. 2f).

Mesenchymal stem cell identification

Both NPS-EMSCs and EMSCs expressed the markers CD44, vimentin, Sox2, and Nestin (Fig. 3a). The quality of mesenchymal stem cells was evaluated based on morphology, surface marker expression, and differentiation potential. NPS-overexpressing EMSCs showed no morphological changes compared with EMSCs (Fig. 3b). The osteogenic and adipogenic differentiation was induced in both cell types using their respective induction media and detected by alkaline phosphatase and Oil Red O staining, respectively. The results indicated that EMSCs and NPS-EMSCs have similar differentiation potential (Fig. 3b).

Characterization of hydrogel scaffolds

Following cell seeding onto the scaffold and in vitro culture, AM/PI staining was used to assess cell survival on days 1, 3, and 5 (Fig. 3c). The results showed that EMSCs adhered to the scaffold and survived, showing an even distribution and growth along the scaffold, with many honeycomb networks observed. The results indicated that hydrogel scaffolds possess excellent biocompatibility, promoting cell proliferation and survival.

The hydrogel exhibited a jelly-like appearance, and SEM analysis revealed a honeycomb network structure within the scaffold (Fig. 3d). The average pore size of the porous 3D structure of the scaffold was 201.29 ± 7.25 μm,

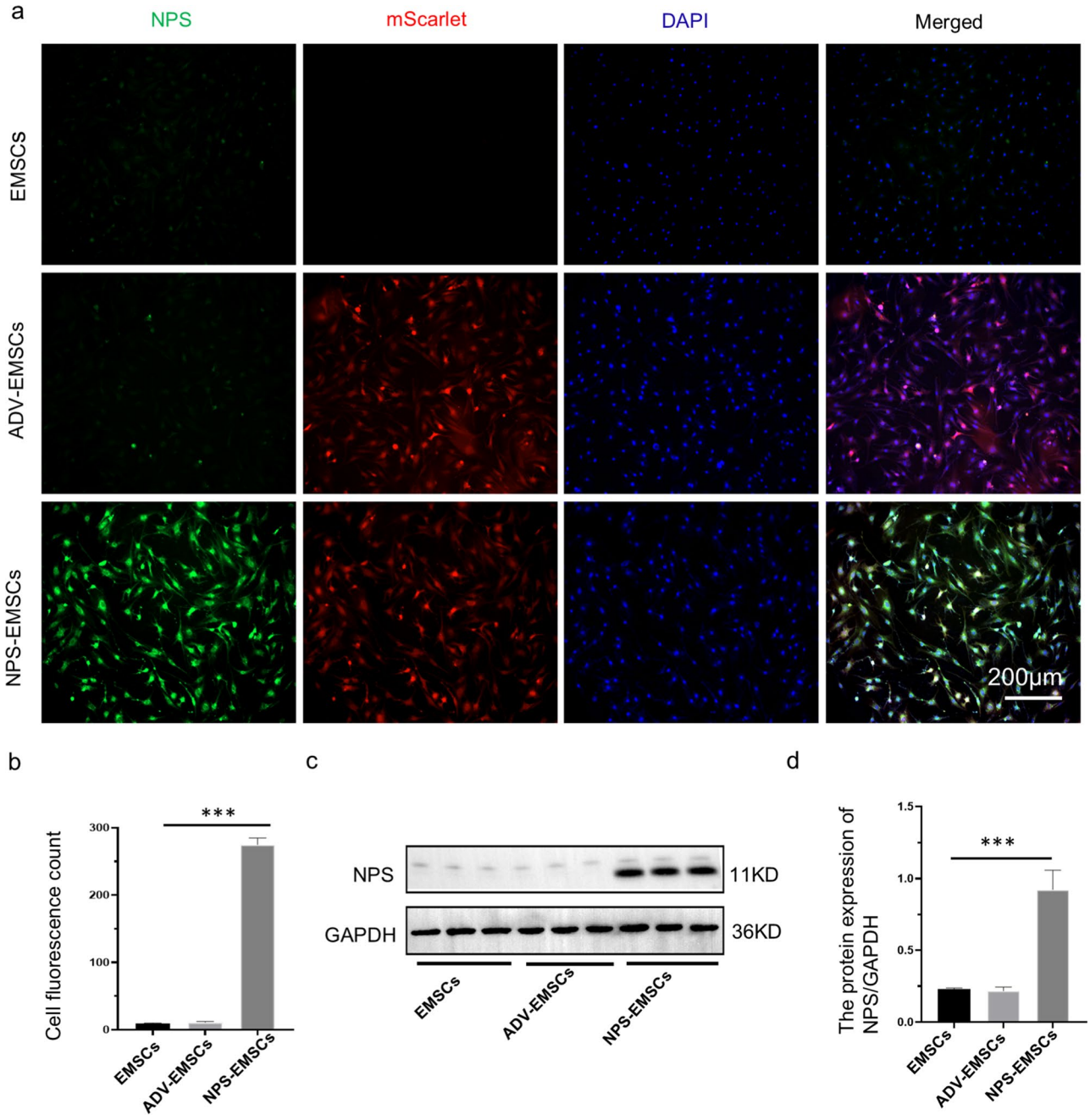

Fig. 1 Expression levels in different EMSCs groups. (**a**) Cellular immunofluorescence staining showing the amount of m-scarlet protein (green and red) expressed in cells from the EMSC, NPS-EMSC groups. (**b**) Statistical analysis. (**c**) Western blot analysis of gene expression in infected and uninfected fetal muscle cells ($n=3$). (**d**) Statistical plot of the results of the Western blot analysis of NPS. * $P<0.05$, ** $P<0.01$, * $P<0.001$, ns: no significant difference

making it suitable as both a carrier of cells and a conduit for nerve regeneration to promote connections after nerve regeneration.

Transplantation of NPS-EMSCs into the injury site can promote motor function recovery in an SCI model

Following complete transection of T8-T9, all rats became paralyzed. The primary goal of SCI treatment is to restore motor functions. The BBB Scale was used to evaluate the recovery after 8 weeks of treatment. Weekly behavioral analyses using the BBB Exercise Scale were conducted with scores shown in Fig. 4b. The BBB scores dropped to 0 across all groups, 1 day post-surgery, confirming the successful establishment of the SCI model. At 8 weeks post-transplantation, the BBB scores in the SCI + NPS-EMSCs group were significantly higher than those in the SCI group ($P<0.05$), indicating improved motor functions in rats following NPS-EMSC treatment. HE staining

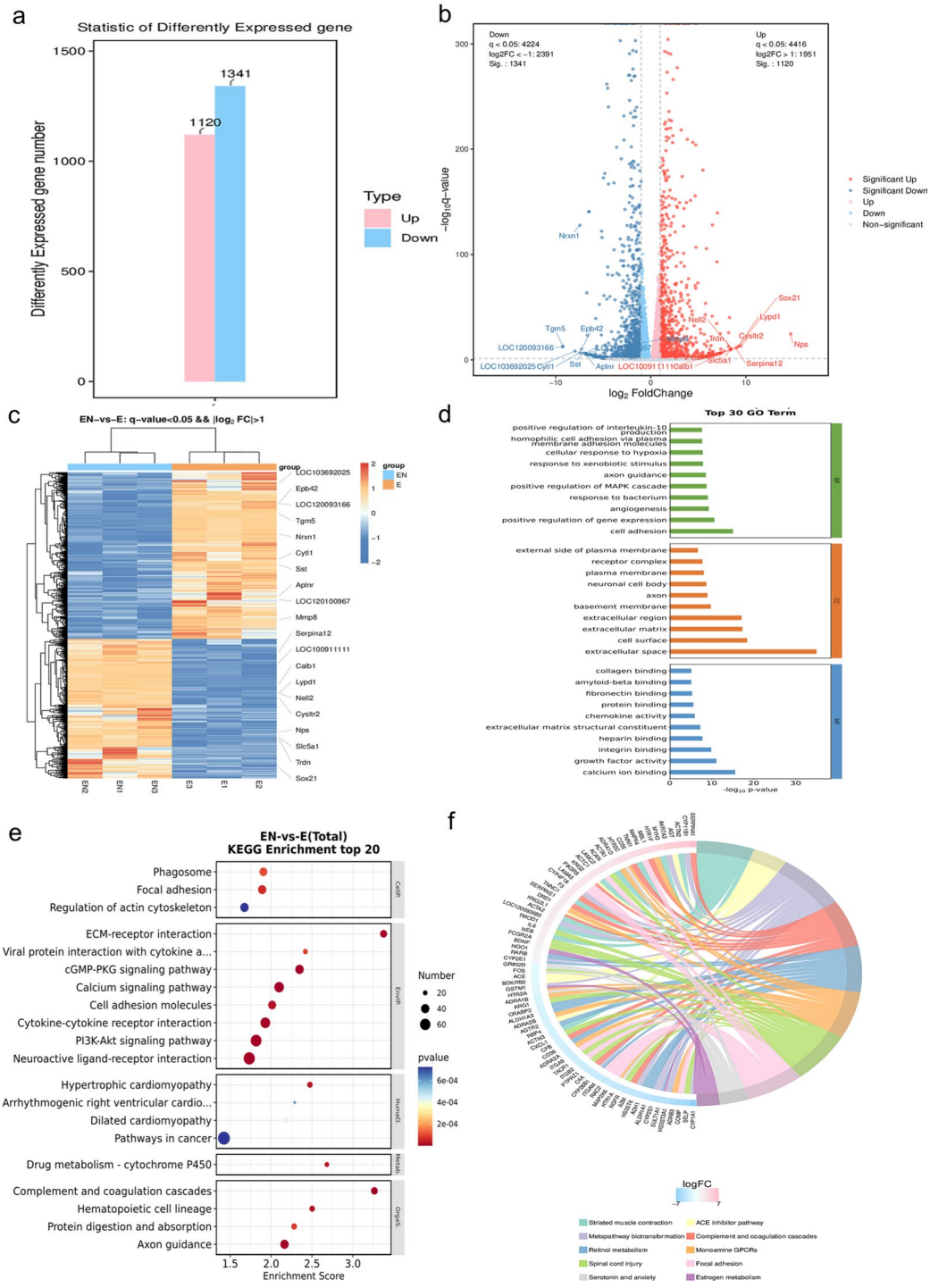

Fig. 2 RNA sequencing reveals changes in cellular gene expression profiles of EMSCs overexpressing NPS. (**a**) RNA gene differential expression map. (**b**) Differential gene volcano map. (**c**) Cluster heatmap of the differentially expressed genes. (**d**) GO enrichment analysis. (**e**) KEGG enrichment assay. (**f**) Wiki Pathway analysis

was used to assess histological changes in the injured spinal cord 12 weeks post-SCI. In the control group, the injured spinal cord tissue structure appeared loose with prominent cavities. The SCI + EMSC group showed more free tissue at the site of injury compared with the SCI + NPS-EMSCs group (Fig. 4c). The SCI + NPS-EMSCs group exhibited the smallest luminal area, suggesting that the NPS-EMSCs group had the most effective integration in the transverse spinal cord.

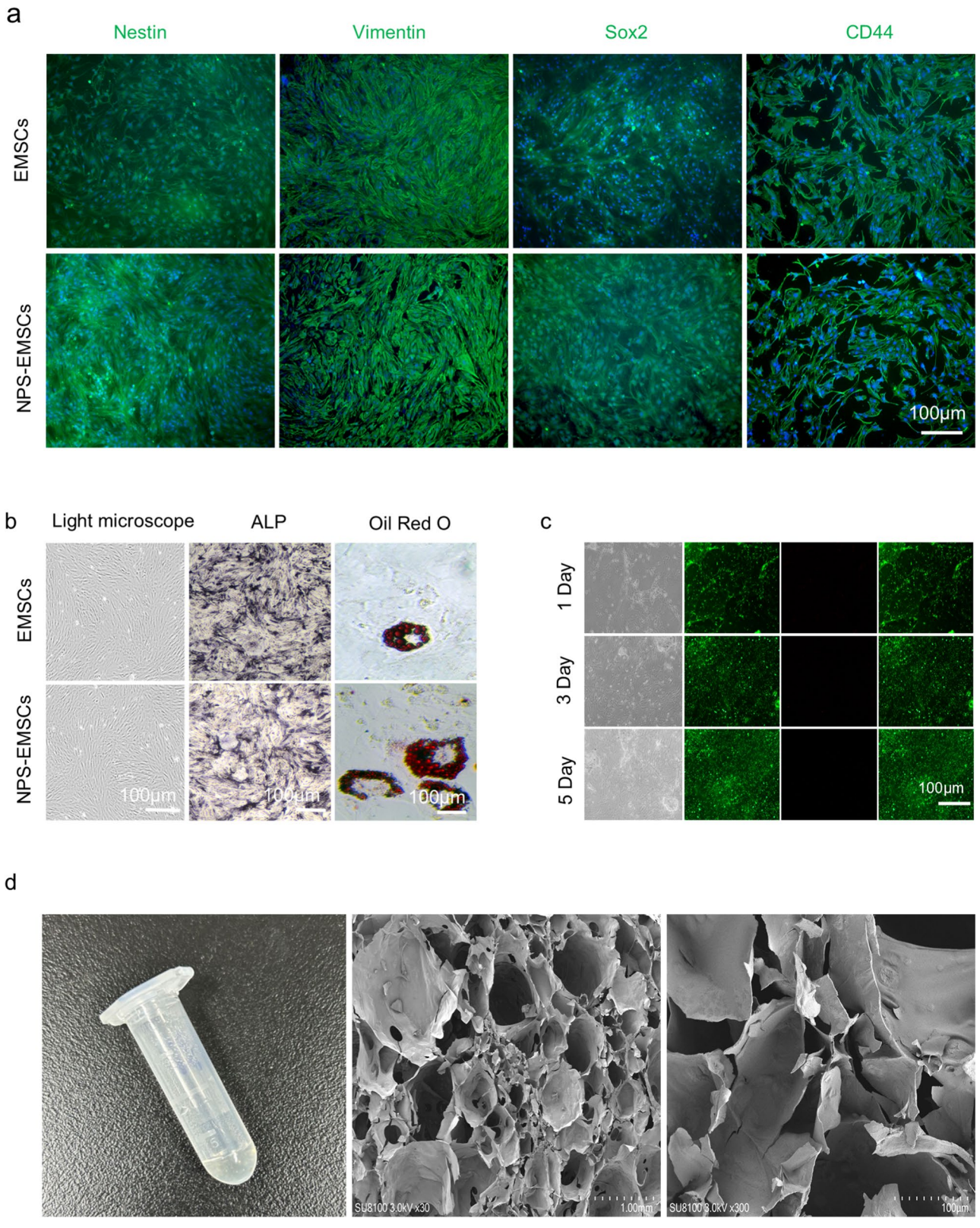

Fig. 3 (See legend on next page.)

(See figure on previous page.)

Fig. 3 Cell culture and identification of stem cells derived from the nasal mucosa of rats. (**a**) Immunofluorescence for positive markers (CD44, vimentin, Sox2, and Nestin) on the surfaces of EMSCs and NPS-EMSCs. Scale bar = 100 μm. (**b**) Phase-contrast microscopy image of EMSCs from primary cultures to the third passage and NPS overexpressing EMSCs. Scale bar = 100 μm; Alkaline phosphatase staining indicates that mesenchymal stem cells derived from the nasal mucosa have osteogenic differentiation ability, and Oil Red O staining reveals that EMSCs have adipose differentiation ability. Scale bar = 20 μm. (**c**) AM/PI double-staining fluorescence images at 1, 3, and 5 days, with green indicating live cells and red indicating dead cells. Scale bar = 100 μm. (**d**) Scanning electron microscopy image of the hydrogel scaffold demonstrating its porous structure

NPS-EMSCs improved the survival rate and migration of cells

Four weeks after injury, m-Scarlet-positive cells were observed throughout the injury site and in both the rostral and caudal regions of the SCI + NPS-EMSCs group under low-power microscopy (Fig. 4d). Western blotting analysis confirmed that the expression of NPS in the SCI + NPS-EMSCs group was significantly higher than in the other groups, consistent with the immunofluorescence findings (Fig. 4e), indicating that NPS-EMSC intervention increased the expression of NPS at the SCI site.

NPS-EMSCs can enhance axonal regeneration in injured tissue after SCI and significantly inhibit axonal regeneration of the glial scar, a crucial step in post-injury tissue repair

To evaluate the potential for axonal regeneration in injured spinal cords treated with NPS-EMSCs, we conducted an immunofluorescence analysis of a key marker (neurofilament NF200, a tissue protein found only in neurons). We examined three parts in each group: the beak, injury zone, and tail. The result revealed regeneration of NF200 axons after treatment with NPS-EMSCs or EMSCs. In the SCI group, the axons were completely lost at the injury center. The number of NF200-positive axons crossing the injured area increased slightly in the SCI + EMSCs group and the SCI + Fibrin group. In contrast, the SCI + NPS-EMSCs treatment group presented with many NF200-positive axons in the middle region of the injury. Additionally, nerve continuity was more pronounced in the SCI + NPS-EMSCs treatment group compared with other groups, indicating axonal growth within the SCI zone (Fig. 5a). These data suggested that SCI + NPS-EMSCs promote axonal growth in injured areas, contributing to the recovery of hind limb function and increasing the possibility of axonal regeneration after SCI. Immunofluorescent staining for GFAP (green) was performed to assess astrocyte distribution following transection. In the control group, astrocytes clumped tightly to form a scar barrier. However, in the SCI + NPS-EMSCs group, astrocytes appeared more permissive, and no significant glial scars were formed to limit axon regeneration (Fig. 5b). As expected, lesions in the SCI + NPS-EMSCs group displayed reduced scarring of GFAP-positive glial cells, suggesting that NPS-EMSCs inhibit astrocytes, thereby creating a more conducive environment for axonal regeneration. Western blot analysis corroborated these findings by showing that the expression of NF200 and GFAP in the SCI + NPS-EMSCs group was significantly higher compared to the SCI group (Fig. 5d, e, f).

Improved myelin regeneration (MBP)

Demyelination is a common pathology that leads to dysfunction in SCI. Myelin basic protein (MBP), a component of the myelin sheath, is essential for nerve impulse conduction along the axons and maintaining myelin stability in the central nervous system. The effect of the intervention on myelination was determined using double immunofluorescence staining for GFAP and MBP in the SCI area (Fig. 6a). In the SCI + NPS-EMSCs group, MBP-positive cells were clearly observed at the injury site but not in the other groups, indicating that NPS-EMSCs treatment promotes myelin regeneration, and the results of GFAP immunostaining are consistent with previous results. NPS-EMSC intervention significantly inhibited GFAP expression.

NPS-EMSCs promote the differentiation of endogenous NSCs

Following SCI, various factors such as spinal nerve cell apoptosis, axonal rupture, glial scarring, and cavity formation significantly hinder neuronal regeneration and repair. Endogenous NSCs have the potential to differentiate into neurons, astrocytes, and oligodendrocytes. Compared with the other two types of differentiation, neurons play a critical role in maintaining normal electrophysiological activities of the body and possess strong self-renewal potential. Nestin is a marker for NSCs that can be used to label NSCs, whereas Tuj-1 is a marker used to identify early neurons.To determine the effect of cells transplanted at the site of SCI on endogenous NSCs, we performed immunofluorescence staining for NSCs and Tuj-1 cells in each group. The results showed that NSCs appeared near the injury site, with significant differences in their numbers across groups. The number of NSCs and Tuj-1 cells in the SCI + NPS-EMSCs group was significantly greater than that in the other groups. More Tuj-1-positive cells were observed near the injured spinal cord in both SCI + NPS-EMSCs and SCI + EMSC groups, with SCI + NPS-EMSCs group having greater number of the cells compared with the SCI + EMSCs group, suggesting that the cultured NSCs differentiated into neurons rather than astrocytes (Fig. 6b). The

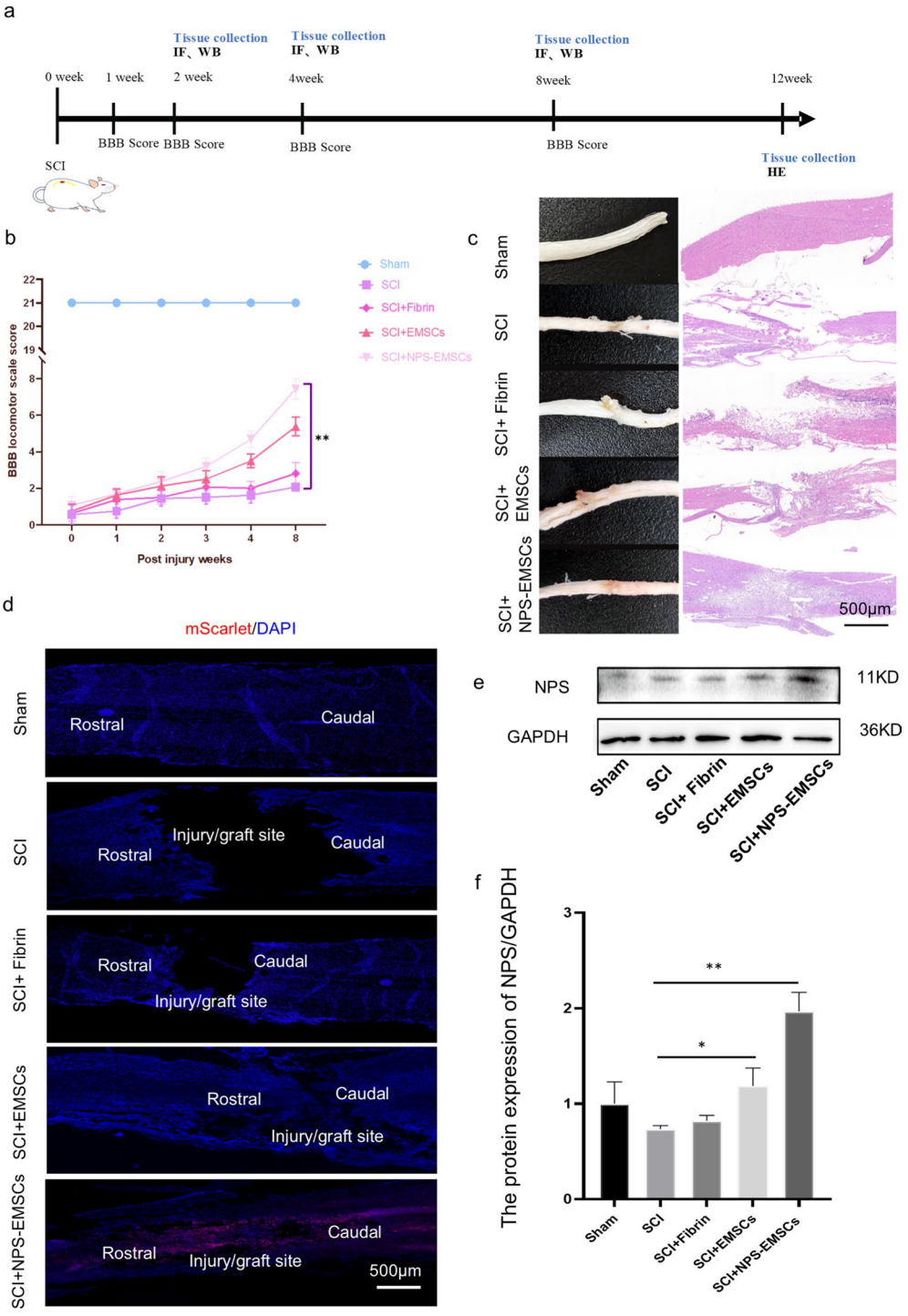

Fig. 4 Histological examination of the graft site 12 weeks after surgery. (**a**) Flow chart of the test design. (**b**) Recovery of motor function; $n = 8$ rats per group. (**c**) Spinal cord tissue stained with hematoxylin and eosin; scale bar = 500 μm. (**d**) Representative immunofluorescence images of gross observations of injured spinal cord segments 4 weeks post-surgery, showing mScarlet distribution throughout the injured spinal cord and highlighting the role of NPS in promoting the survival and migration of EMSCs-derived cells in vivo. Red fluorescent protein-positive (mScarlet) cells are derived from transplanted NPS-EMSCs; scale bar = 500 μm. (**e**) Western blot analysis of NPS expression at the injury site($n = 6$). (**f**) Statistical plot of the results of the Western blot analysis of NPS. * $P < 0.05$, ** $P < 0.01$, *** $P < 0.001$, ns: no significant difference

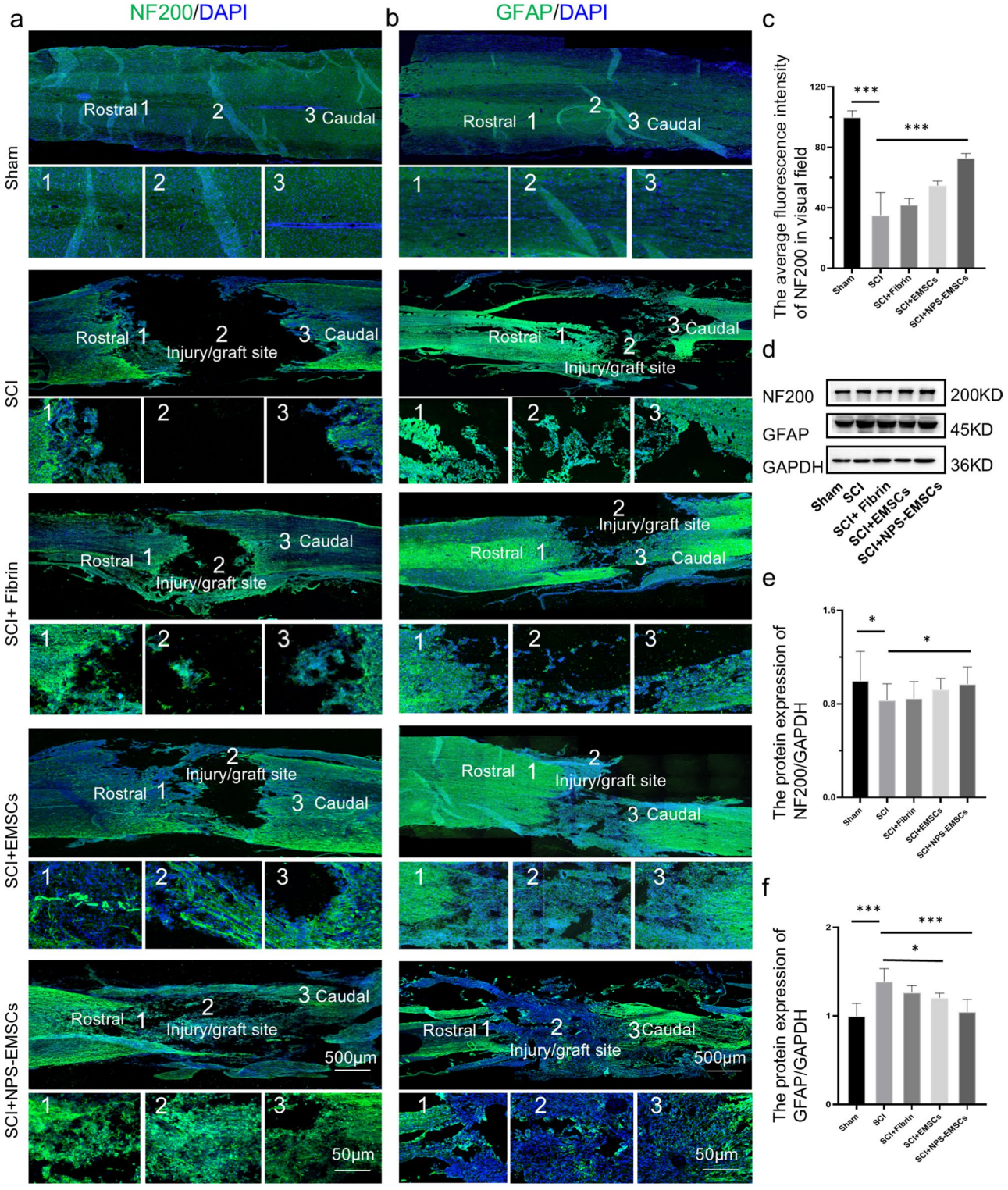

Fig. 5 Hydrogels overexpressing NPS-EMSCs promote axon growth and inhibit astrocyte activity. (**a**) NF200 immunofluorescence staining shows the profile of spinal cord segments in each group. NF200-positive axons (green) significantly extend into the rostral 1, injured 2, and caudal 3 regions near the injured site, clearly showing the distribution of the axons, indicating that NPS-EMSCs promote the extension of NF200-positive axons to the injured site. Scale bar = 500 μm. Higher magnification in the middle box area shows superimposed images of NF200- and DAPI-marked objects; scale bar = 50 μm($n = 3$). (**b**) Schematic diagram of GFAP (green) immunofluorescence staining results; scale bar = 500 μm. The digital area shows an overlay image of GFAP- and DAPI-labeled objects at higher magnification. (**c**) Statistical plot of the mean NF200 fluorescence intensity. (**d**) Western blot analysis of NF200 and GFAP expression at the injury site ($n = 6$);. (**e**, **f**) Statistical plot of the results of the Western blot analysis of NF200 and GFAP. * $P < 0.05$, ** $P < 0.01$, *** $P < 0.001$, ns: no significant difference

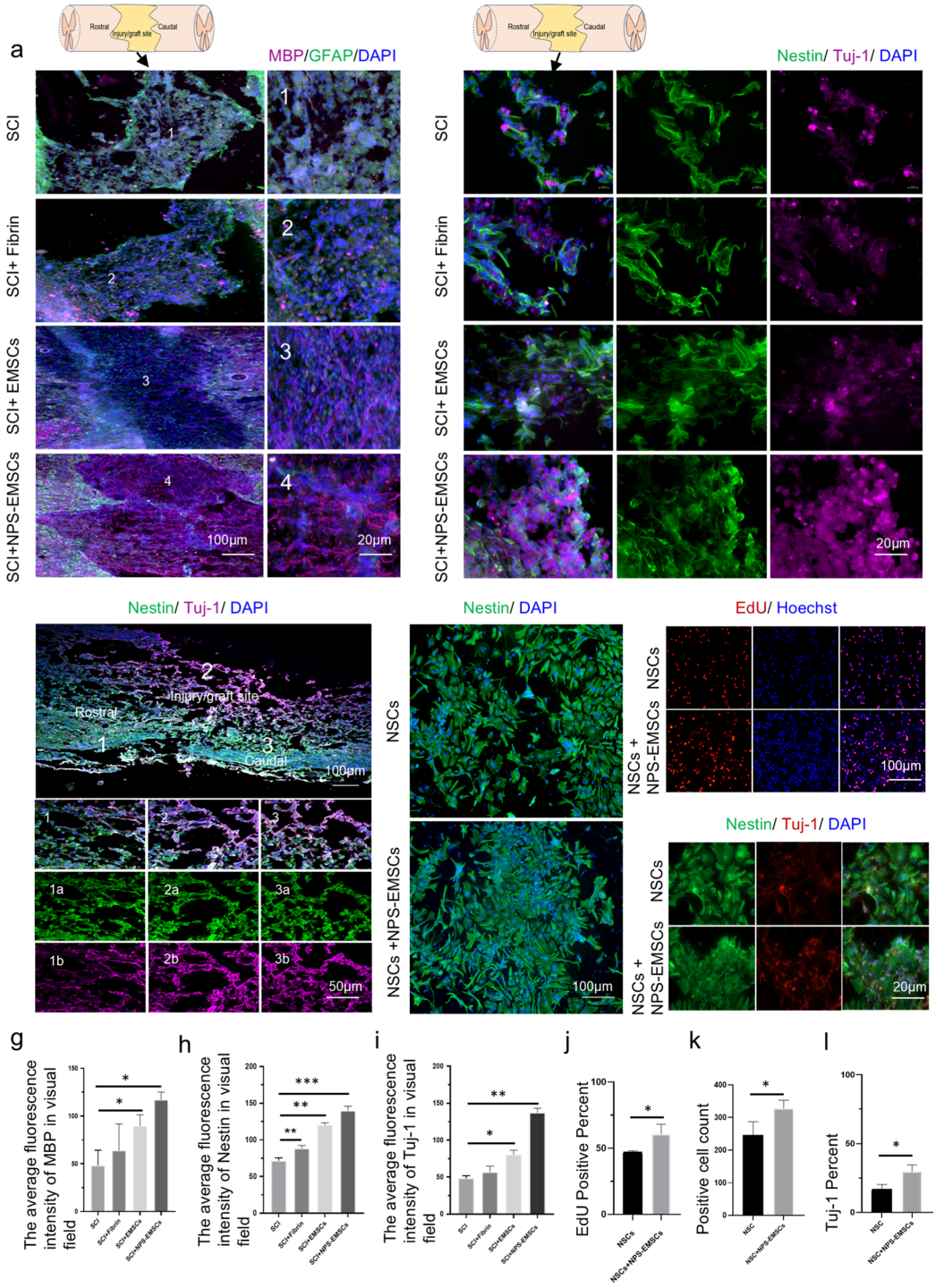

Fig. 6 (See legend on next page.)

staining results also revealed the presence of NSCs and neurons in both the beak and tail of the spinal cord after SCI, indicating that NSCs recruit neurons and differentiate at injury sites, regardless of treatment. Nestin immunofluorescence staining revealed that the NPS-EMSCs recruited more NSCs to the injury site. Additionally, we conducted longitudinal cross-sectional staining in the SCI + NPS-EMSCs group and found that immunofluorescence staining for Nestin and Tuj-1 revealed more Tuj-1-positive cells in the SCI + NPS-EMSCs group compared with the injured spinal cord and tail, indicating the presence of more nascent neurons in the injured spinal cord (Fig. 6c).To further investigate whether NPS-EMSCs promoted the proliferation of endogenous NSCs,

(See figure on previous page.)

Fig. 6 NPS-EMSCs protect the myelin sheath and improve regeneration of the spinal cord in rats following SCI. NPS-EMSC treatment significantly inhibits glial scarring and myelin sheath growth from the host spinal cord to the injured site. (**a**) Horizontal sections subjected to MBP (purple) and GFAP (green) immunofluorescence show the distribution of MBP. Scale bar = 100 μm. Higher magnification in the middle box area shows superimposed images of MBP-, GFAP- and DAPI-marked objects; scale bar = 20 μm($n = 3$). (**b**) Immunofluorescence staining results of Nestin (green) and Tuj-1 (purple) in the SCI area of each experimental group; scale bar = 20 μm. (**c**) Immunofluorescence staining of Nestin (green) and Tuj-1 (purple) in longitudinal sections from the SCI + NPS-EMSCs group with high magnification in the middle box, showing overlay images of Nestin, Tuj-1, and DAPI-labeled objects; scale bar = 100 μm; 50 μm in the middle box. (**d**) Immunofluorescence staining of NSCs cultured with NPS-EMSC alone or indirectly, Nestin (green), scale bar = 100 μm. (**e**) EdU staining of NSCs cultured with NPS-EMSC alone or indirectly; scale bar = 100 μm. (**f**) NSCs cultured alone and indirectly with NSCs, showing differentiation into neurons with immunostaining for Nestin (green) or Tuj-1 (red); scale bar = 20 μm. (**g**) Statistical plot of the mean MBP fluorescence intensity. (**h**) Statistical analysis of the mean fluorescence intensity of Nestin in Tuj-1 cells. (**i**) Statistical analysis of the mean fluorescence intensity of Tuj-1. (**j**) EdU staining statistics for NSCs cultured alone and indirectly with NPS-EMSCs. (**k**) Statistical analysis of NSC proliferation cultured with NPS-EMSCs alone and indirectly. (**l**) Tuj-1 immunofluorescence statistics for NSCs cultured with NPS-EMSCs alone and indirectly. * $P < 0.05$, ** $P < 0.01$, *** $P < 0.001$, ns: no significant difference

we isolated NSCs and co-cultured them indirectly with NPS-EMSCs. After successfully extracting and indirectly incubating NSCs for 7 days, we fixed the cells for immunofluorescence analysis. Almost all NSCs expressed Nestin, with the NPS-EMSC-NSCs group exhibiting a significantly higher level of Nestin compared with the NSCs cultured alone (Fig. 6d, j). Similarly, the proportion of EdU was significantly higher in the NPS-EMSC-NSCs group than in the NSCs-only group (Fig. 6e, j). These results indicated that NPS-EMSCs increased the number and promoted the proliferation of the NSCs. Next, we investigated whether NPS-EMSCs promoted NSCs differentiation. After 10 days of indirect co-culture, the cells were fixed and subjected to immunofluorescence analysis. The result revealed a significant increase in Tuj-1 cells in the presence of NPS-EMSCs (Fig. 6f, l), indicating that NPS-EMSCs indeed promoted neuronal differentiation of NSCs.

NPS-EMSCs modulate neurotrophic factors to promote nerve regeneration

Neurotrophin-3 (NT-3) plays a crucial role in the regenerative microenvironment of the spinal cord. It helps prevent the death of injured spinal cord neurons and maintain their survival while also improving axonal regeneration. To further elucidate the potential role of NPS-EMSCs in neural regeneration, NT-3 expression was assessed using immunofluorescence and western blotting techniques. In the fourth week, the immunofluorescence results indicated that the expression level of the NT-3 protein in the spinal cord tissue of rats treated with NPS-EMSCs was significantly higher than that observed in the SCI group (Fig. 7a). This finding suggests more a greater quantity of is released from the SCI site following NPS-EMSC treatment, thus thereby facilitating regeneration. Western blot analysis corroborated these findings by showing that the expression of NT-3 in the SCI + NPS-EMSCs group was significantly higher compared to the SCI group (Fig. 7b, c), suggesting that the transplanted cells secrete more NT-3 during the repair of SCI. To further verify whether NPS-overexpressing EMSCs secreted more NT-3, we performed immunofluorescence staining on cultured EMSCs and NPS-EMSCs, revealing that NPS-overexpressing EMSCs secreted more NT-3 (Fig. 7d), which was also verified by western blot analysis (Fig. 7e, f, g).

Activating the PI3K/AKT/GSK3β pathway to promote neural regeneration

Spinal cord samples were collected subsequent to examine the underlying mechanisms of repair. Based on the results of the KEGG enrichment analysis (Fig. 2e), we identified genes that are differentially expressed between NPS-EMSCs and EMSCs, which are involved in the PI3K/AKT signaling pathway. The AKT signaling pathway has recently been implicated in a variety of cellular functions, including cell growth, reproduction, and differentiation. Western blot analysis demonstrated a significant increase in the phosphorylation levels of PI3K, AKT, and GSK3β in the SCI + NPS-EMSCs group. This finding suggests that NPS-EMSCs facilitate the proliferation and neuronal differentiation of NSCs by activating the PI3K/AKT/GSK3β phosphorylation pathway (Fig. 8c). To further elucidate the mechanism by which NPS-EMSCs facilitate neuronal differentiation in vitro, we evaluated the phosphorylation levels of AKT and GSK3β in NSCs, and it was determined whether they activate the AKT-GSK3β signaling pathway. MK2206, an inhibitor of the AKT signaling pathway, was employed to inhibit the phosphorylation of AKT and GSK3β that was induced by conditioned medium. Immunofluorescence staining was performed to evaluate the proliferation (Fig. 8a) and neuronal differentiation (Fig. 8b) of NSCs following preconditioning. These results revealed that the differentiation of NSCs decreased following MK2206 pretreatment, indicating that NPS-EMSCs promote NSC proliferation and neuronal differentiation by activating the PI3K/AKT/GSK3β signaling pathway.

Discussion

Currently, there is no effective treatment for SCI, which can result in the loss of motor function and significantly diminish the quality of life for affected individuals [36, 37]. Growing evidence indicates that mesenchymal stem

cells offer advantages in repairing injured spinal cord by reducing inflammation, secreting nerve growth and neurotrophic factors, and promoting axonal regeneration and neural pathway reconstruction [6, 7, 38]. EMSCs have unique advantages compared with the current study of embryonic stem cells for the treatment of SCI. First, embryonic stem cells are derived from embryos, and their acquisition typically involves the destruction of early embryos, which is not only technically challenging but also raises ethical concerns. On the contrary, EMSCs can be safely biopsied with local anesthetic, which makes them suitable for autologous transplantation, reducing the risk of immune rejection post-transplantation [39, 13, 14]. Thus, the EMSC is a more acceptable option for researchers and clinicians concerned about ethical implications [40]. Second, EMSCs can be expanded in vitro using standard cell culture techniques, making them a more practical option for large-scale production and clinical application.

According to prior studies, mesenchymal stem cells can be integrated with growth factors, various cell types, pharmacological agents, and biological scaffolds to attain effective clinical therapeutic outcomes. Genetically modified seed cell therapy is emerging as a promising approach for the treatment of enhancing the functionality of seed cells or employing these cells to deliver therapeutic agents [41, 42]. Our results suggest that NPS-overexpression EMSCs promote axonal regeneration after SCI in rats. One of the three main findings of our study is that NPS-EMSCs recruited NSCs and promoted their differentiation into neurons, as evidenced by an increased number of NSCs near the injury site. More Tuj-1-positive cells were observed near the injury site in the NPS-EMSC intervention group (Fig. 6b), and immunostaining for Nestin and Tuj-1 revealed elevated levels of NSCs and immature neuron expression, respectively, in the NPS-EMSC-treated group than in the control group. GFAP is specifically expressed in astrocytes as a cytoskeletal component [43], and its expression increases in activated astrocytes, leading to the production of multiple proinflammatory cytokines after SCI [44]. GFAP immunofluorescence staining revealed that the NPS-overexpressing group had the lowest GFAP expression levels (Fig. 6a). The results further confirmed that NPS-EMSC intervention reduced GFAP-positive cells (Fig. 5b, d), suggesting that recruited NSCs differentiated into neurons rather than glial cells at the injury site. These findings indicate that transplanted NPS-EMSCs are instrumental in the neuronal differentiation of endogenous NSCs while simultaneously fostering a supportive microenvironment for neurogenesis. This process may facilitate the re-establishment of neuronal relays, thereby reconnecting isolated neural networks and enhancing the efficient transmission of neural signals in areas of damage.

Axonal regeneration is crucial for the establishment of neural connections, with myelin serving a significant role in facilitating axonal signaling and maintenance [45–47]. MBP immunofluorescence analysis revealed greater axonal remyelination intensity in the NPS-EMSC group 8 weeks post-surgery, compared with other groups (Fig. 6a). Additionally, rats transplanted with NPS-EMSCs showed more nerve fibers compared with other treatment groups. This study demonstrated that NF-200, an axonal marker, exhibited higher expression in the NPS-EMSC-transplanted group compared to the other groups (Fig. 5a), suggesting that these neuron-associated proteins may also originate from the differentiation of endogenous NSCs.

The second major finding of our study focused on how NPS-EMSCs enhance neuronal differentiation of NSCs. We performed RNA sequencing analysis of EMSCs before and after gene modification and found that the KEGG enrichment of NPS-modified EMSCs affected the PI3K/Akt pathway. Prior studies have shown that activation of the PI3K/Akt/GSK3β pathway promotes neuronal differentiation in NSCs but not glial differentiation [48, 49].

We conducted both in vitro and in vivo experiments to validate our findings. Our results indicate that NPS-EMSC treatment enhances the proliferation and neuronal differentiation of NSCs, contributing to improved treatment outcomes. Endogenous NSCs are crucial as they serve as the formation of astrocytes within glial scars, contribute to the maintenance of tissue integrity, provide neurotrophic support to surviving neurons, and represent potential therapeutic targets for the treatment of SCI [50, 51]. The PI3K/AKT signaling pathway plays an important role in all types of neural cells, including the growth, metabolism, proliferation, survival, differentiation, and apoptosis of glial cells and neurons. Phosphorylation of GSK3β inhibits the activity of the GSK3β protein, which is a major downstream molecule in the PI3K/AKT pathway.

This signaling pathway is primarily activated by a variety of biological factors, which subsequently triggers a cascade of downstream signaling molecules that produce various biological effects [52]. In spinal cord repair, activation of the PI3K/AKT signaling pathway promotes endothelial cell survival, reduces neural damage, and mitigates inflammatory cell death [53, 54]. We observed that the proliferation and neuronal differentiation of NSCs co-cultured with NPS-EMSCs were reduced by AKT inhibitor pretreatment in vitro. In vivo, treatment with NPS-EMSCs increased PI3K, Akt, and GSK3β phosphorylation levels in spinal cord tissue after SCI. These results suggest that NPS-EMSCs promote NSC proliferation and neuronal differentiation through the PI3K-Akt-GSK3β

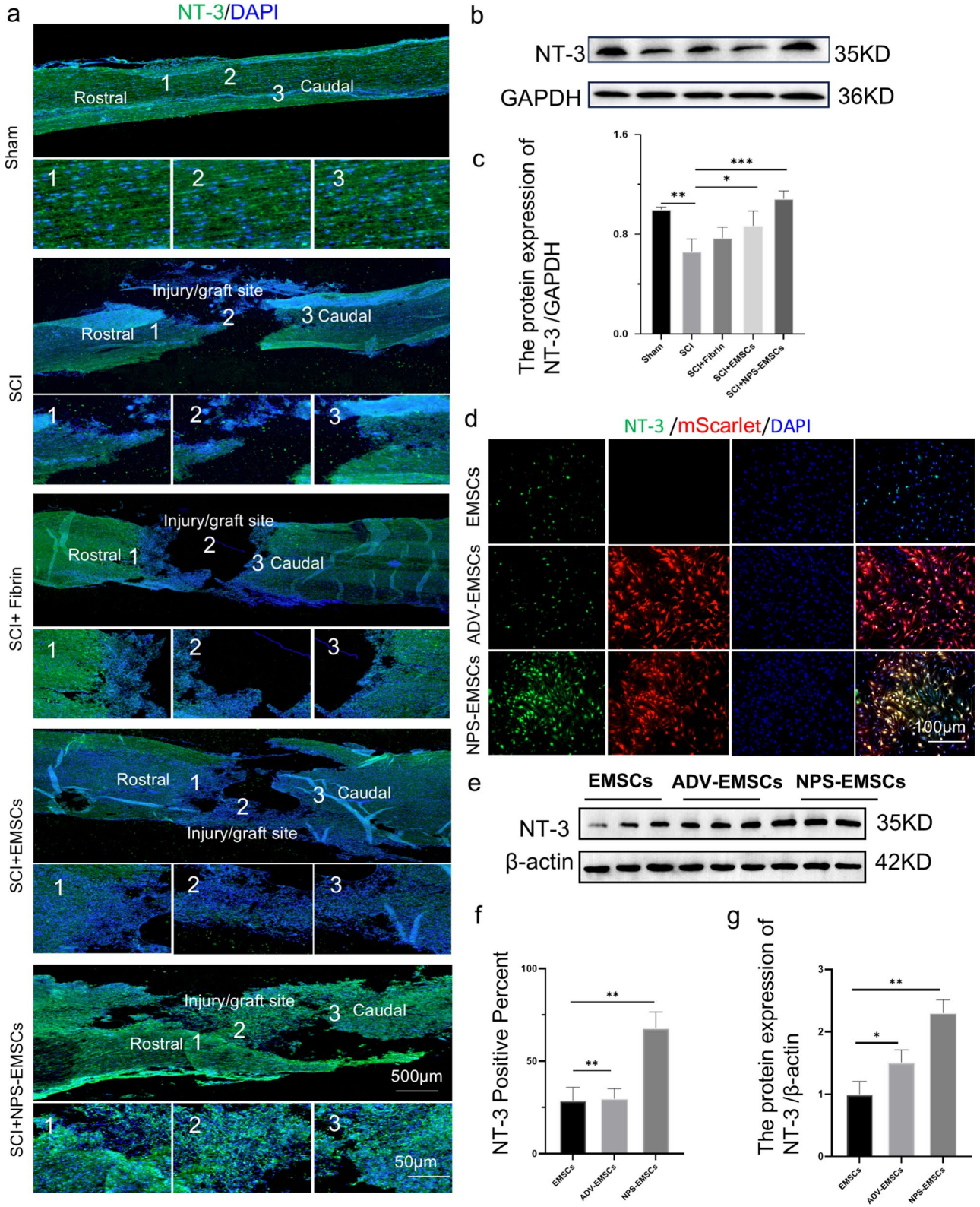

Fig. 7 Protective effect of NPS-EMSCs on neurons and the expression of neurotrophic factors following SCI in rats. (**a**) Representative images of NT-3 immunofluorescence staining after SCI. NT-3 (green), DAPI (blue), scale bar = 500 μm. (**b**) Western blot results for NT-3 in the spinal cord tissue($n=6$). (**c**) Western blot statistics of NT-3 in spinal cord tissue. (**d**) Immunofluorescence staining of NT-3 in EMSCs and NPS-EMSCs. (**e**) Western blot results for NT-3 expression in EMSCs and NPS-EMSCs ($n=3$). (**f**) Statistics of the NT-3 immunofluorescence staining results for EMSCs and NPS-EMSCs. (**g**) Western blot results for NT-3 in in EMSCs and NPS-EMSCs. * $P<0.05$, ** $P<0.01$, *** $P<0.001$, ns: no significant difference

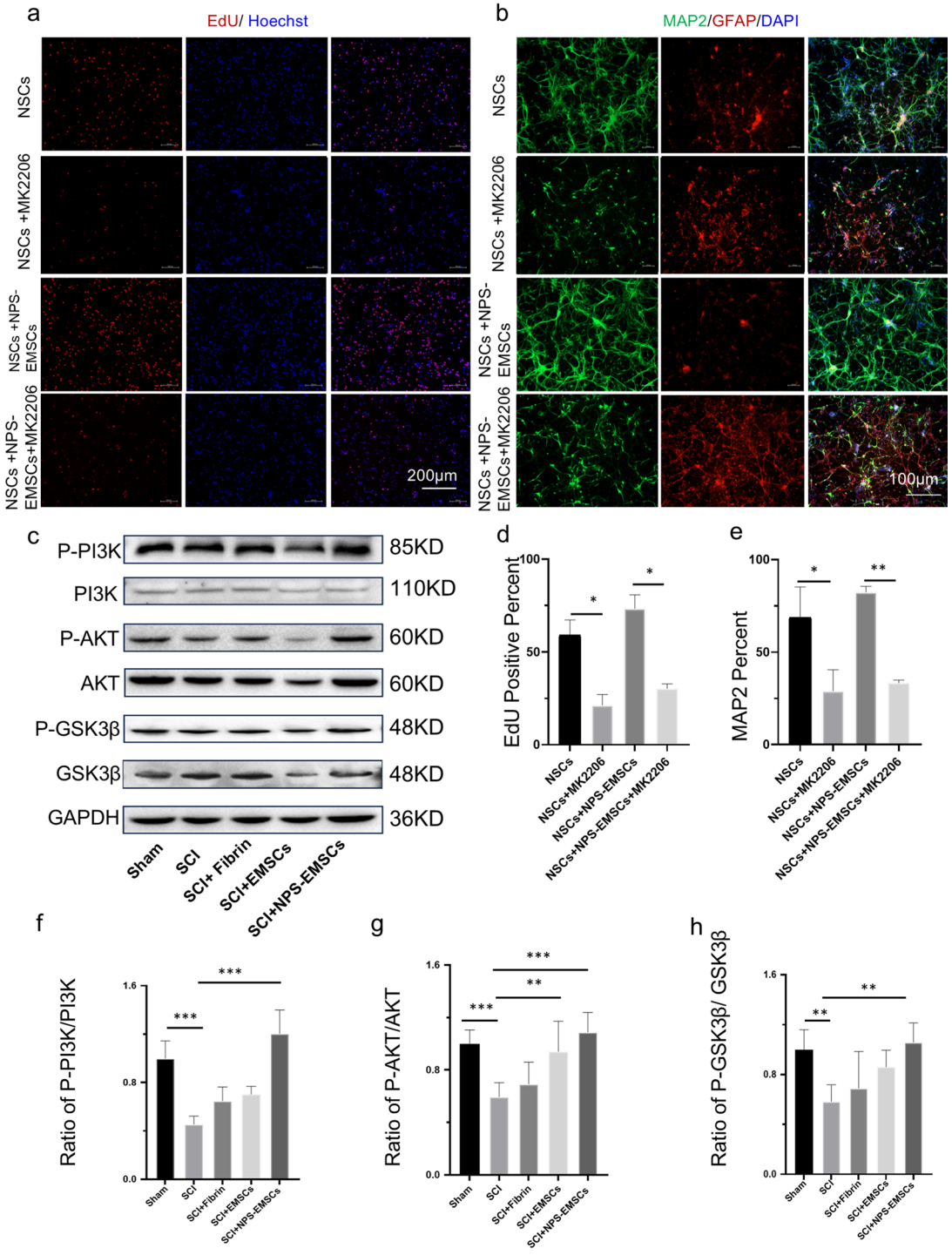

Fig. 8 NPS-EMSCs promote NSC proliferation and neuronal differentiation by activating the PI3K/AKT/GSK3β signaling pathway. (**a**) EdU staining of MK2206-pretreated NSCs co-cultured with NPS-EMSCs. Scale bar = 50 μm. (**b**) Immunofluorescence staining of MAP2 (green) and GFAP (red) in MK2206-pretreated NSCs co-cultured with NPS-EMSCs; scale bar = 50 μm. (**c**) Western blot analysis of PI3K, AKT, and GSK3β phosphorylation levels in rats with SCI($n = 6$). (**d**) Statistical analysis of EdU-positive cells. (**e**) Statistics for MAP2 (green)-positive cell. (**f-h**) Statistical analysis of PI3K, AKT, and GSK3β phosphorylation levels. * $P < 0.05$, ** $P < 0.01$, *** $P < 0.001$, ns: no significant difference

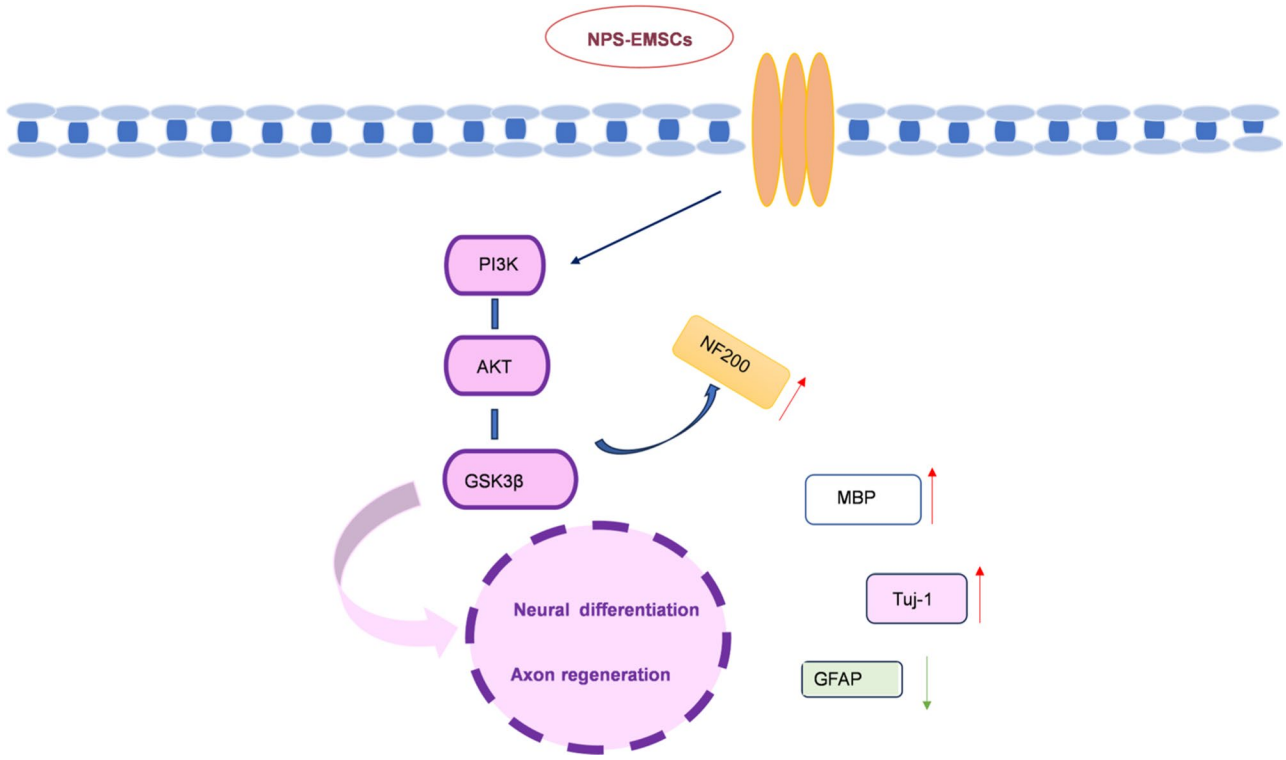

Fig. 9 The beneficial effects of NPS-EMSCs on neuronal development

pathway, significantly enhancing the therapeutic outcome of SCI in rats (Fig. 9).

Functional recovery is an important indicator of SCI treatment efficacy and is the ultimate goal of clinical treatment [55]. As expected, rats implanted with NPS-EMSCs showed a significant increase in BBB scores, reflecting the best recovery of motor function. The BBB scores were evaluated at 1-, 2-, 4-, and 8-weeks post-operation, and the results revealed that untreated rats experienced significant deterioration in BBB scores, injury morphology, and spinal cord pathological, whereas the NPS-EMSC group exhibited significantly higher BBB scores, and injury morphology and pathological changes were alleviated. NPS-EMSC treatment provided an enhanced protective effect against SCI, as evidenced by improved BBB scores after injury. Furthermore, the overexpression of NPS-EMSCs amplified their positive effects on lesion morphology and significantly improved motor function.

The presence of extracellular inhibitory factors and the lack of neurotrophic factors are the main reasons for reduced axonal regeneration following SCI [56, 57, 58]. Our third major finding revealed that NPS-modified EMSCs produced higher levels of neurotrophic factors than control EMSCs, with a significant increase in NT-3 expression in spinal cord tissue following NPS-EMSC treatment (Fig. 7a). Neurotrophic factors are small molecular proteins synthesized by target cells and transported retrogradely to neuronal cell bodies via neurites. Their primary functions are to maintain the survival of neurons during embryonic development, promote their differentiation, induce axonal growth, regulate the physiological functions of mature neurons, and promote the repair of injured neurons. Studies have shown that in vitro cultured and isolated EMSCs secrete neurotrophic factors. These factors, which include NT-3, play a vital role in the development and growth of neurons [59–61].

This study suggests that NPS-EMSCs enhance the neural regeneration microenvironment in myelopathy by promoting neurotrophic factor expression and functional recovery. Our results demonstrate for the first time that implanting NPS-EMSCs into T8-T9 injury sites represents a promising therapeutic approach. NPS-modified EMSCs effectively promote NSC proliferation, increase neurotrophic factor secretion, and improve the neuronal differentiation of NSCs. Overexpressing NPS-EMSCs in combination with hydrogels can enhance the BBB scores in SCI rats, alleviate associated pathological changes, promote nerve remyelination and axonal growth, inhibit astrocyte scar formation, and promote motor function recovery. These findings suggest substantial potential for clinical application.

This study had some limitations. (1) There were some challenges in translating the treatment into clinical practice, such as the scalability of EMSC production and safety concerns related to genetic modification.

Therefore, safety concerns regarding the genetic modifications made to EMSCs need to be addressed to ensure patient safety; (2) the repair mechanisms of EMSCs in the treatment of SCI were not fully studied. Further research is necessary to better understand the repair mechanisms; and (3) the cell quality, dose, surgical indications, contraindications, and safety and efficacy evaluation systems in our study were not fully standardized. Future clinical applications require standardization of these critical factors. Although EMSCs have shown great potential in the treatment of SCI, their clinical application necessitates extensive long-term exploration to confirm their effectiveness and safety.

Conclusion

In this study, we observed that NPS may positively influence neuronal development. The overexpression of NPS in EMSCs resulted in significant improvements in treatment outcomes, including reduced glial scar formation, improved neurogenesis, and increased motor function recovery in hind limbs. The observed effects seem to be associated with the augmented proliferation and differentiation of NSCs through the activation of the PI3K/Akt/GSK3β signaling cascade, accompanied by a decrease in the astrocyte population. Further studies are required to validate these findings. Furthermore, transplantation of NPS-modified EMSCs could enhance tissue repair and facilitate motor function recovery after SCI. Our results strongly support the feasibility and effectiveness of NPS-modified EMSCs for clinical applications.

Abbreviations

SCI	Spinal Cord Injury
EMSCs	Nasal Mucosal Mesenchymal Stem Cells
NPS	Neuropeptide S
NPSR	Neuropeptide S Receptor
SD	Sprague-Dawley
NSC	Neural Stem Cell
NT-3	Neurotrophin-3
BBB	Basso, Beattie, and Bresnahan (scoring system)

Supplementary Information

The online version contains supplementary material available at https://doi.org/10.1186/s13287-025-04250-4.

Supplementary Material 1

Acknowledgements

The authors express their gratitude to Wentao Shi, a doctoral candidate at Jiangnan University; Yan Zou, a doctoral candidate at Nanjing University; and Dr. Liping Shen from the Wuxi Institute of Neurosurgery for their invaluable assistance in the experimental research, which is not included in the final manuscript. Additionally, the authors acknowledge the financial support provided by the Wuxi Institute of Neurosurgery. The authors declare that no AI-generated content has been utilized in the preparation of this manuscript.

Author contributions

The study was designed by Xiaojie Lu, Yazhuo Zhang, Bai Xu, and Xudong Zhao. Yazhuo Zhang and Xiaojie Lu provided contributions in research review, study design assistance, and key consultation. Animal experiments were conducted by Wenhui Yang, Mengyuan Yu, and Yushi Tang. The cell experiments were performed by Yilu Li, Zhenxing Tao, Yushi Tang, and Cuiping Sun. Microscopic examinations were carried out by Wenhui Yang and Yushi Tang. Data analysis was performed by Yilu Li, Yushi Tang, Zhenxing Tao, and Yang Ye. The manuscript was written and edited by Wenhui Yang, with contributions from Yilu Li and Yushi Tang. Xiaojie Lu supervised and guided the research process.

Funding

This work was supported by the National Natural Science Foundationof China (No. 82071381 and 82072791); Jiangsu Provincial Science and Technology Plan Project BK20231051; The Research and Development Plan of Jiangsu Province (Social Development) BE2022695; The Fund of "the Fourteenth Five-Year Plan" of Jiangsu Provincial Medical Key Discipline ZDXK202227; The Fund of Wuxi Medical Key Discipline ZDXK2021004.

Data availability

The datasets used and analysed during the current study are available from the corresponding author on reasonable request. The RNA-sequencing data has been uploaded to NCBI's Gene Expression Omnibus (GEO) and can be accessed by public (https://www.ncbi.nlm.nih.gov/geo/query/ acc. cgi?acc=GSE280779). All data generated or analyzed in this study are included in this article.

Declarations

Ethics approval

All experimental animal procedures were approved by the Committee of Experimental Animals of Jiangnan University and were conducted according to the guidelines of the China Council on Animal Care and Use. Approved Project Title: Neuropeptide S Combined with EMSCs in Spinal Cord Injury Recovery. Approval number: JN. No20230315S0720829[062]. Approval date: 15 March 2023.All possible efforts were devoted to minimizing pain and discomfort in the animals.

Competing interests

The authors declare that they have no competing interests.

Author details

[1]Neuroscience Center, Wuxi School of Medicine, Jiangnan University, Wuxi, Jiangsu Province 214122, PR China
[2]Department of Neurosurgery, Jiangnan University Medical Center, Wuxi, Jiangsu Province 214122, PR China
[3]Wuxi Neurosurgical Institute, Wuxi, Jiangsu Province 214122, PR China
[4]Pharmaceutical Department, Inner Mongolia Forestry General Hospital, Hulunbuir, Inner Mongolia Autonomous Region 022150, PR China
[5]Beijing Neurosurgical Institute, Capital Medical University, Beijing 100070, PR China

Received: 23 August 2024 / Accepted: 20 February 2025
Published online: 28 February 2025

References

1. Anjum A, Yazid MDi, Fauzi Daud M, Idris J, Ng AMH, Selvi Naicker A et al. Spinal cord injury: pathophysiology, multimolecular interactions, and underlying recovery mechanisms. Int J Mol Sci. 2020;21(20).
2. Chiba Y, Kuroda S, Maruichi K, Osanai T, Hokari M, Yano S, et al. Transplanted bone marrow stromal cells promote axonal regeneration and improve motor function in a rat spinal cord injury model. Neurosurgery. 2009;64(5):991–1000.
3. Peng Ding ZY, Weimin Wang J, Wang L, Xue. Transplantation of bone marrow stromal cells enhances infiltration and survival of CNP and Schwann cells to promote axonal sprouting following complete transection of spinal cord in adult rats. Am J Transl Res. 2014. https://pmc.ncbi.nlm.nih.gov/articles/PMC4058305/
4. Lin L, Lin H, Bai S, Zheng L, Zhang X. Bone marrow mesenchymal stem cells (BMSCs) improved functional recovery of spinal cord injury partly by promoting axonal regeneration. Neurochem Int. 2018;115:80–4.

5. Yu Li P-PS, Wang B. Induced pluripotent stem cell technology for spinal cord injury: a promising alternative therapy. Neural Regeneration Res. 2021;16(8).
6. Gazdic M, Volarevic V, Harrell C, Fellabaum C, Jovicic N, Arsenijevic N et al. Stem cells therapy for spinal cord injury. Int J Mol Sci. 2018;19(4).
7. Sun G, Li G, Li D, Huang W, Zhang R, Zhang H, et al. HucMSC derived exosomes promote functional recovery in spinal cord injury mice via attenuating inflammation. Mater Sci Engineering: C. 2018;89:194–204.
8. Shao A, Tu S, Lu J, Zhang J. Crosstalk between stem cell and spinal cord injury: pathophysiology and treatment strategies. Stem Cell Res Ther. 2019;10(1).
9. Bingnan W, Jiao T, Ghorbani A, Baghei S. Enhancing regenerative potential: A comprehensive review of stem cell transplantation for sports-related neuronal injuries, with a focus on spinal cord injuries and peripheral nervous system damage. Tissue Cell. 2024;88:102429.
10. Chen Q, Zhang Z, Liu J, He Q, Zhou Y, Shao G et al. A fibrin matrix promotes the differentiation of EMSCs isolated from nasal respiratory mucosa to myelinating phenotypical Schwann-like cells. (0219–1032 (Electronic)). https://doi.org/10.14348/molcells.2015.2170
11. Li YA-O, Cao X, Deng W, Yu Q, Sun C, Ma P et al. 3D printable sodium alginate-Matrigel (SA-MA) hydrogel facilitated Ectomesenchymal stem cells (EMSCs) neuron differentiation. (1530–8022 (Electronic)). https://doi.org/10.1177/0885328220961261
12. Hauser S, Widera D, Qunneis F, Müller J, Zander C, Greiner J, et al. Isolation of novel multipotent neural Crest-Derived stem cells from adult human inferior turbinate. Stem Cells Dev. 2011;2012/03(20):742–56.
13. Ao Q, Wang Aj Fau - Chen GQ, Chen G, Fau - Wang SJ, Zhang XF, Zhang XF. Combined transplantation of neural stem cells and olfactory ensheathing cells for the repair of spinal cord injuries. (0306–9877 (Print)). https://doi.org/10.1016/j.mehy.2007.04.011
14. Prockop DJ. Repair of tissues by adult stem/progenitor cells (MSCs): controversies, Myths, and changing paradigms. (1525-0024 (Electronic)).
15. Liu J, Chen Q, Fau - Zhang Z, Zhang Z, Fau - Zheng Y, Zheng Y, Fau - Sun X, Sun X, Fau - Cao X, Cao X, Fau - Gong A et al. Fibrin scaffolds containing Ectomesenchymal stem cells enhance behavioral and histological improvement in a rat model of spinal cord injury. (1422–6421 (Electronic)).
16. Shafiee A, Kabiri M, Fau - Ahmadbeigi N, Ahmadbeigi N, Fau - Yazdani SO, Yazdani So Fau -, Mojtahed M, Mojtahed M, Fau - Amanpour S, Amanpour S, Fau - Soleimani M et al. Nasal septum-derived multipotent progenitors: a potent source for stem cell-based regenerative medicine. (1557–8534 (Electronic)). https://doi.org/10.1089/scd.2010.0420
17. Yu QA-O, Liao M, Sun C, Zhang Q, Deng W, Cao XA-O et al. LBO-EMSC hydrogel serves a dual function in spinal cord injury restoration via the PI3K-Akt-mTOR Pathway. (1944–8252 (Electronic)).
18. Deng W, Shao F, He Q, Wang Q, Shi W, Yu Q et al. EMSCs build an All-in-One niche via Cell-Cell lipid raft assembly for promoted neuronal but suppressed astroglial differentiation of neural stem cells. (1521–4095 (Electronic)). https://doi.org/10.1002/adma.201806861
19. Wang X, Hong CG, Duan R, Pang ZL, Zhang MN, Xie HA-O et al. Transplantation of olfactory mucosa mesenchymal stromal cells repairs spinal cord injury by inducing microglial polarization. (1476–5624 (Electronic)). https://doi.org/10.1038/s41393-024-01004-6
20. Sahni V, Kessler JA. Stem cell therapies for spinal cord injury. Nature Reviews Neurology. https://doi.org/10.1038/nrneurol.2010.73
21. Hwang SJ, Cho TH, Kim IS, Kim IS. In vivo gene activity of human mesenchymal stem cells after scaffold-mediated local transplantation. (1937-335X (Electronic)). https://doi.org/10.1089/ten.TEA.2013.0507
22. Handy CR, Krudy C, Fau - Boulis N, Boulis N. Gene therapy: a potential approach for cancer pain. (2090– 1550 (Electronic)). https://doi.org/10.1155/2011/987597
23. Mao B. [Research status and prospects of gene therapy in spinal cord injuries]. (1002–892 (Print)). https://pubmed.ncbi.nlm.nih.gov/10437103/
24. Sato S, Shintani Y, Miyajima N, Yoshimura K. Novel G protein-coupled receptor protein and DNA thereof. World Patent Application; 2002.
25. Xu Y-L, Reinscheid RK, Huitron-Resendiz S, Clark SD, Wang Z, Lin SH, et al. Neuropept S Neuron. 2004;43(4):487–97.
26. Reinscheid RK. Phylogenetic appearance of Neuropeptide S precursor proteins in tetrapods. 2007.
27. Reinscheid RK, Neuropeptide S. Anatomy, pharmacology, genetics and physiological functions. 2008.
28. Akçalı İ, Akkan SS, Bülbül M. The regulatory role of central neuropeptide-S in locomotion. Peptides. 2023 2023/12/01/;170:171110. https://doi.org/10.1016/j.peptides.2023.171110
29. Li W, Chang M, Peng Y-L, Gao Y-H, Zhang J-n, Han R-W, et al. Neuropeptide S produces antinociceptive effects at the supraspinal level in mice. Regul Pept. 2009;156(1–3):90–5.
30. Zhang Z, He Q, Deng W, Chen Q, Hu X, Gong A, et al. Nasal Ectomesenchymal stem cells: Multi-lineage differentiation and transformation effects on fibrin gels. Biomaterials. 2015;49:57–67.
31. Anders S, Pyl PT, Huber W. HTSeq–a Python framework to work with high-throughput sequencing data. (1367–4811 (Electronic)). https://doi.org/10.1093/bioinformatics/btu638
32. The Gene Ontology Resource. 20 years and still GOing strong. (1362–4962 (Electronic)).
33. Kanehisa M, Araki M, Fau - Goto S, Goto S, Fau - Hattori M, Hattori M, Fau - Hirakawa M, Hirakawa M, Fau - Itoh M, Itoh M, Fau - Katayama T et al. KEGG for linking genomes to life and the environment. (1362–4962 (Electronic)). https://doi.org/10.1093/nar/gkm882
34. Huang F, Gao T, Wang W, Wang L, Xie Y, Tai C et al. Engineered basic fibroblast growth factor-overexpressing human umbilical cord-derived mesenchymal stem cells improve the proliferation and neuronal differentiation of endogenous neural stem cells and functional recovery of spinal cord injury by activating the PI3K-Akt-GSK-3β signaling pathway. (1757–6512 (Electronic)). https://doi.org/10.1186/s13287-021-02537-w
35. D. Michele Basso MSB. and Jacqueline C. Bresnahan. A Sensitive and Reliable Locomotor Rating Scale for Open Field Testing in Rats. 1995.
36. Zeng CA-O. Advancing spinal cord injury treatment through stem cell therapy: A comprehensive review of cell types, challenges, and emerging technologies in regenerative medicine. LID– 10.3390/ijms241814349 [doi] LID– 14349. (1422-0067 (Electronic)). https://doi.org/10.3390/ijms241814349
37. Kumar R, Lim J, Mekary RA, Rattani A, Dewan MC, Sharif SY, et al. Traumatic spinal injury: global epidemiology and worldwide volume. World Neurosurg. 2018;113:e345–63.
38. Shao A, Tu S, Lu J, Zhang J. Crosstalk between stem cell and spinal cord injury: pathophysiology and treatment strategies. Stem Cell Res Ther. 2019;10(1):238.
39. Alizadeh R, Kamrava SK, Bagher Z, Farhadi M, Falah M, Moradi F et al. Human olfactory stem cells: As a promising source of dopaminergic neuron-like cells for treatment of Parkinson's disease. (1872–7972 (Electronic)). https://doi.org/10.1016/j.neulet.2018.12.011
40. Girard SD, Devéze A, Fau - Nivet E, Nivet E, Fau - Gepner B, Gepner B, Fau -. Roman FS, Roman Fs Fau - Féron F, Féron F. Isolating nasal olfactory stem cells from rodents or humans. LID– 2762 [pii] LID– 10.3791/2762 [doi]. (1940-087X (Electronic)). https://doi.org/10.3791/2762
41. Myers TJ, Granero-Molto F, Longobardi L, Li T, Yan Y, Spagnoli A. Mesenchymal stem cells at the intersection of cell and gene therapy. Expert Opin Biol Ther. 2010;10(12):1663–79.
42. Shen R, Lu Y, Cai C, Wang Z, Zhao J, Wu Y et al. Research progress and prospects of benefit-risk assessment methods for umbilical cord mesenchymal stem cell transplantation in the clinical treatment of spinal cord injury. Stem Cell Res Ther. 2024;15(1).
43. Kanno H, Pressman Y, Moody A, Berg R, Muir EM, Rogers JH, et al. Combination of engineered Schwann cell grafts to secrete neurotrophin and chondroitinase promotes axonal regeneration and locomotion after spinal cord injury. J Neurosci. 2014;34(5):1838–55.
44. Yin X, Yin Y, Cao FL, Chen YF, Peng Y, Hou WG, et al. Tanshinone IIA attenuates the inflammatory response and apoptosis after traumatic injury of the spinal cord in adult rats. PLoS ONE. 2012;7(6):e38381.
45. Günther MI, Weidner N, Müller R, Blesch A. Cell-seeded alginate hydrogel scaffolds promote directed linear axonal regeneration in the injured rat spinal cord. Acta Biomater. 2015;27:140–50.
46. Cao Z, Yao S, Xiong Y, Zhang Z, Yang Y, He F, et al. Directional axonal regrowth induced by an aligned fibrin nanofiber hydrogel contributes to improved motor function recovery in canine L2 spinal cord injury. J Mater Sci Mater Med. 2020;31(5):40.
47. Lai BQ, Bai YR, Han WT, Zhang B, Liu S, Sun JH, et al. Construction of a niche-specific spinal white matter-like tissue to promote directional axon regeneration and myelination for rat spinal cord injury repair. Bioact Mater. 2022;11:15–31.
48. Park SY, Park J, Sim SH, Sung MG, Kim KS, Hong BH, et al. Enhanced differentiation of human neural stem cells into neurons on graphene. Adv Mater. 2011;23(36):H263–7.
49. Ceto S, Sekiguchi KJ, Takashima Y, Nimmerjahn A, Tuszynski MH. Neural stem cell grafts form extensive synaptic networks that integrate with host circuits after spinal cord injury. Cell Stem Cell. 2020;27(3):430–e405.

50. Stenudd M, Sabelström H, Frisén J. Role of endogenous neural stem cells in spinal cord injury and repair. JAMA Neurol. 2015;72(2):235–7.
51. Li C, Luo Y, Li S. The roles of neural stem cells in Myelin regeneration and repair therapy after spinal cord injury. Stem Cell Res Ther. 2024;15(1):204.
52. Dou MY, Wu H, Zhu HJ, Jin SY, Zhang Y, He SF. Remifentanil preconditioning protects rat cardiomyocytes against hypoxia-reoxygenation injury via δ-opioid receptor mediated activation of PI3K/Akt and ERK pathways. Eur J Pharmacol. 2016;789:395–401.
53. Shultz RB, Zhong Y. Minocycline targets multiple secondary injury mechanisms in traumatic spinal cord injury. Neural Regen Res. 2017;12(5):702–13.
54. Abbaszadeh F, Fakhri S, Khan H. Targeting apoptosis and autophagy following spinal cord injury: therapeutic approaches to polyphenols and candidate phytochemicals. Pharmacol Res. 2020;160:105069.
55. Chen K, Yu W, Zheng G, Xu Z, Yang C, Wang Y, et al. Biomaterial-based regenerative therapeutic strategies for spinal cord injury. NPG Asia Mater. 2024;16(1):5. 2024/01/19.
56. Ruschel J, Hellal F, Flynn KC, Dupraz S, Elliott DA, Tedeschi A, et al. Axonal regeneration. Systemic administration of epothilone B promotes axon regeneration after spinal cord injury. Science. 2015;348(6232):347–52.
57. O'Donovan KJ. Intrinsic axonal growth and the drive for regeneration. Front Neurosci. 2016;10:486.
58. Dell'Anno MT, Strittmatter SM. Rewiring the spinal cord: direct and indirect strategies. Neurosci Lett. 2017;652:25–34.
59. Wang Z, Duan H, Hao F, Hao P, Zhao W, Gao Y et al. Circuit reconstruction of newborn neurons after spinal cord injury in adult rats via an NT3-chitosan scaffold. (1873–5118 (Electronic)). https://doi.org/10.1016/j.pneurobio.2022.102375
60. Barde YA, Edgar D, Thoenen H. Purification of a new neurotrophic factor from mammalian brain. Embo J. 1982;1(5):549–53.
61. Pollock K, Dahlenburg H, Nelson H, Fink KD, Cary W, Hendrix K, et al. Human mesenchymal stem cells genetically engineered to overexpress Brain-derived neurotrophic factor improve outcomes in Huntington's disease mouse models. Mol Ther. 2016;24(5):965–77.

Publisher's note